

## **Distribution Agreement**

In presenting this thesis as a partial fulfillment of the requirements for a degree from Emory University, I hereby grant to Emory University and its agents the non-exclusive license to archive, make accessible, and display my thesis in whole or in part in all forms of media, now or hereafter now, including display on the World Wide Web. I understand that I may select some access restrictions as part of the online submission of this thesis. I retain all ownership rights to the copyright of the thesis. I also retain the right to use in future works (such as articles or books) all or part of this thesis.

Yifei Wu

April 3, 2025

Investigating Histone Acetylation in Lipogenic Triple Negative Breast Cancer Cells using Cell Engineering and Bioinformatics

By

Yifei Wu

Karmella Haynes  
Adviser

Biology

Karmella Haynes  
Adviser

Patrick Cafferty  
Committee Member

Rabindra Tirouvanziam  
Committee Member

2025

Investigating Histone Acetylation in Lipogenic Triple Negative Breast Cancer Cells using Cell  
Engineering and Bioinformatics

By

Yifei Wu

Karmella Haynes  
Adviser

An abstract of  
a thesis submitted to the Faculty of Emory College of Arts and Sciences  
of Emory University in partial fulfillment  
of the requirements of the degree of  
Bachelor of Science with Honors

Biology

2025

## Abstract

Investigating Histone Acetylation in Lipogenic Triple Negative Breast Cancer Cells using Cell Engineering and Bioinformatics  
By Yifei Wu

Triple negative breast cancer (TNBC) is an aggressive breast cancer subtype that has poor outcomes when compounded with obesity. Adipocyte secreted factors (ASFs) activate metabolic pathways that change the level of acetyl-CoA, a substrate involved in histone acetylation and fatty acid synthesis, suggesting an association between epigenetic remodeling and ASFs. Although aberrant histone acetylation is a marker for cancer progression, the relationship between lipogenesis and histone acetylation is yet to be elucidated in TNBC cells. To investigate the association between chromatin structure and tumor suppressor gene (TSG) expression, we used RNA-seq and ATAC-seq to identify if chromosomal accessibility is reduced around the promoter site of downregulated TSGs in lipogenic TNBC cells. We found no significant difference in peak signal value between cells treated with adipocyte-conditioned media (ACM) vs unconditioned media (UCM), suggesting an alternative mechanism for downregulation of TSGs other than chromosomal accessibility. By performing transcription factor enrichment analysis, we found that downregulated TSGs are regulated by a set of TFs that uniquely regulates downDEGs. This suggests downregulation of TSGs is induced by dysregulation of TFs. In future work, we will determine how TNBC aggressiveness is impacted by TFs by treating cells with specific TF inhibitors. To visualize histone acetylation level and nuclear distribution in lipogenic TNBC cells, we use fusion protein technology to engineer plasmids that express histone acetylation reader probes with bromodomain (BRD) dimers fused to fluorescent proteins. We found that BT549 transfection rate with the engineered plasmids was low, likely due to transgene silencing induced by CMV promoter in the GGDestX4 expression vector. In future experiments, we will engineer a new Golden Gate compatible plasmid based on the pSBtetTA-YP\_CFP vector, which has been shown to achieve high transfection rate in BT549 cells. To determine histone acetylation level and its nuclear redistribution in lipogenic TNBC cells, we will re-do transfection with the new expression vector and treat the cells with ACM or UCM.

Investigating Histone Acetylation in Lipogenic Triple Negative Breast Cancer Cells using Cell Engineering and Bioinformatics

By

Yifei Wu

Karmella Haynes

Adviser

A thesis submitted to the Faculty of Emory College of Arts and Sciences  
of Emory University in partial fulfillment  
of the requirements of the degree of  
Bachelor of Science with Honors

Biology

2025

### Acknowledgements

I would like to send my sincere gratitude to my research advisor Dr. Karmella Haynes, who have supported and guided me through the past two years of my research journey, and I have grown so much as a researcher under her mentorship. I would like to thank my graduate mentor Ashley Townsel, who gave me so much encouragement and helped me become a better scholar. I would like to thank Dr. Curtis Henry, one of the most supportive and kindest advisors I've met. I would like to thank Dr. Patrick Cafferty, who have supported me so much since my first year at Emory. I would like to thank all members in the Haynes lab and Henry lab, who have been so kind to me and helped me build my path to biomedical engineering.

Finally, I would like to thank myself for putting in so much effort despite all the challenges. I wish myself best luck at Boston and I know I will achieve great things.

## Table of Contents

Abstract.....	1
Background.....	2
Hypothesis.....	6
Research aims.....	6
Methodology.....	7
Results.....	9
Conclusion and Future Directions.....	19
References.....	22

## **Investigating Histone Acetylation in Lipogenic Triple Negative Breast Cancer Cells using Cell Engineering and Bioinformatics**

### **Abstract**

Triple negative breast cancer (TNBC) is an aggressive breast cancer subtype that has poor outcomes when compounded with obesity. Adipocyte secreted factors (ASFs) activate metabolic pathways that change the level of acetyl-CoA, a substrate involved in histone acetylation and fatty acid synthesis, suggesting an association between epigenetic remodeling and ASFs. Although aberrant histone acetylation is a marker for cancer progression, the relationship between lipogenesis and histone acetylation is yet to be elucidated in TNBC cells. To investigate the association between chromatin structure and tumor suppressor gene (TSG) expression, we used RNA-seq and ATAC-seq to identify if chromosomal accessibility is reduced around the promoter site of downregulated TSGs in lipogenic TNBC cells. We found no significant difference in peak signal value between cells treated with adipocyte-conditioned media (ACM) vs unconditioned media (UCM), suggesting an alternative mechanism for downregulation of TSGs other than chromosomal accessibility. By performing transcription factor enrichment analysis, we found that downregulated TSGs are regulated by a set of TFs that uniquely regulates downDEGs. This suggests downregulation of TSGs is induced by dysregulation of TFs. In future work, we will determine how TNBC aggressiveness is impacted by TFs by treating cells with specific TF inhibitors. To visualize histone acetylation level and nuclear distribution in lipogenic TNBC cells, we use fusion protein technology to engineer plasmids that express histone acetylation reader probes with bromodomain (BRD) dimers fused to fluorescent proteins. We found that BT549 transfection rate with the engineered plasmids was low, likely due to

transgene silencing induced by CMV promoter in the GGDestX4 expression vector. In future experiments, we will engineer a new Golden Gate compatible plasmid based on the pSBtetTA-YP\_CFP vector, which has been shown to achieve high transfection rate in BT549 cells. To determine histone acetylation level and its nuclear redistribution in lipogenic TNBC cells, we will re-do transfection with the new expression vector and treat the cells with ACM or UCM.

## **Background**

As of 2018, the obesity prevalence rate of US adults aged 20 and older is over 40%<sup>1</sup>. Considered an epidemic<sup>2</sup>, obesity is closely associated with an increased risk of at least 13 types of cancer, including breast cancer<sup>3</sup>. Each year, around 2.1 million women are diagnosed with breast cancer worldwide<sup>4</sup>. Among all breast cancer subtypes, triple-negative breast cancer (TNBC) accounts for 10-20% of all breast cancers and is associated with poor prognosis, high rate of recurrence, and low survival rate<sup>5</sup>. It is reported that premenopausal women with obesity (BMI  $\geq 30$  kg/m<sup>2</sup>) have a 42% higher risk of developing TNBC compared with women with normal weight<sup>6</sup>. However, it is worth noting that obesity, as defined by BMI, does not always have a negative impact on TNBC patient outcome. Based on a study on the effect of BMI on survival outcomes of TNBC patients, moderately obese patients have better survival than severely obese, slightly obese, overweight, and underweight/normal weight patients<sup>7</sup> (**Figure 1**). This finding is known as the “obesity paradox in cancer”. Therefore, it is necessary to take into account other confounding factors that might impact patient outcome, such as race, tumor type, and weight history<sup>8</sup>. In breast cancer patients with obesity, adipocyte secreted factors (ASF) have been shown to promote breast cancer epithelial-mesenchymal transition (EMT), invasion, proliferation, and

lipogenesis in invasive cells<sup>910</sup>. Therefore it is important to identify intracellular factors that respond to ASF signaling and mediate intracellular changes that promote cancer. We prepared adipocyte-conditioned media (ACM) as our in-vitro co-culture obesity model (**Figure 2A**). Our preliminary studies have shown that ACM increases lipid droplet formation in BT549 TNBC cells compared to cells treated with unconditioned media (UCM) (**Figure 2B**). Compared to other traditional models of obesity<sup>1110</sup>, our in-vitro co-culture model creates a system where cancerous cells are directly exposed to secreted factors from adipocytes, while maintaining cell-cell interaction. Moreover, such a model allows for a more controlled and precise simulation of the obese microenvironment, since we are able to decide the amount of ACM treatment for the cells.

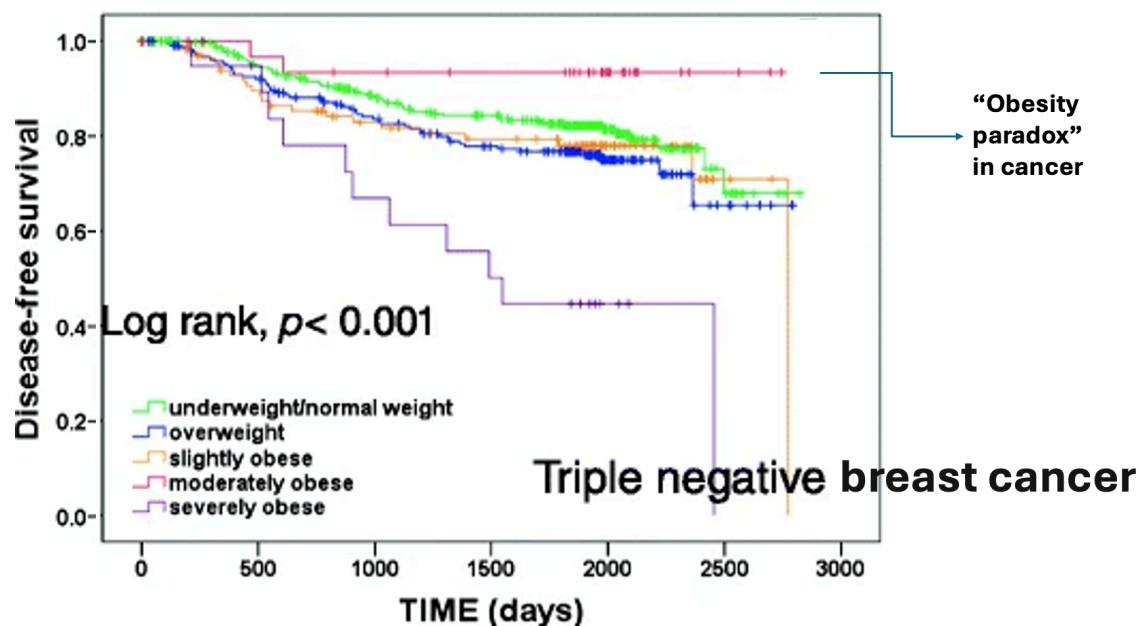


**Figure 1. Kaplan-Meier plot of disease-free survival for TNBC patients based on BMI groups.** Moderately obese TNBC patients have higher survival outcomes than other BMI groups. Figure adapted from Widschwendter et al.<sup>7</sup>

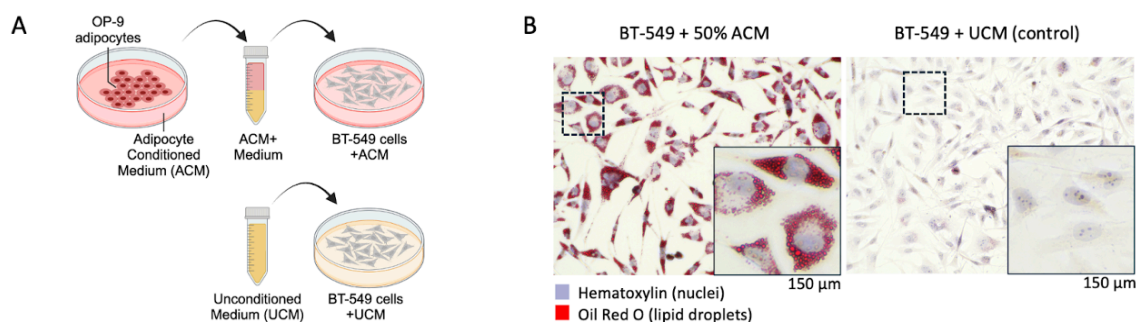


**Figure 2. In-vitro model to study how obesity impacts breast cancer cells.** (A) OP-9 mouse adipocytes are differentiated *in vitro*, the supernatant is collected as adipocyte-conditioned media (ACM) and added to BT549 cells. (B) ACM increases lipid droplet formation in BT549 cells.

Histone acetylation is an epigenetic modification where histone acetyltransferase enzymes (HATs) use acetyl-CoA as substrate to add acetyl groups to histone lysines, decreasing the binding between nucleosome and DNA, and thus activating gene expression<sup>12</sup>. Adipocyte signaling activates pathways including PI3K/AKT/mTOR<sup>13</sup>, NF- $\kappa$ B<sup>14</sup>, JAK/STAT3<sup>15</sup>, hypoxia-induced HIF-1 $\alpha$ <sup>16</sup>, and MAPK/ERK<sup>17</sup>, activating genes that drive metabolic processes, including fatty acid synthesis. In the *de novo* fatty acid (FA) synthesis pathway, acetyl-CoA is converted to malonyl-CoA by acetyl-CoA carboxylase 1 (ACC1) for lipogenesis<sup>18</sup>, suggesting an association between lipogenesis and histone acetylation<sup>19</sup> (**Figure 3**). Aberrant histone acetylation is one of the most pervasive epigenetic drivers that promote breast cancer progression<sup>20</sup>. However, to our knowledge, the association between histone acetylation and lipogenesis in TNBC cells is yet to be elucidated. Therefore, we are interested in determining how histone acetylation might

modulate chromatin in lipogenic TNBC cells, which may shed light on how ASF-stimulated chromatin reorganization contributes to cancer aggressiveness.

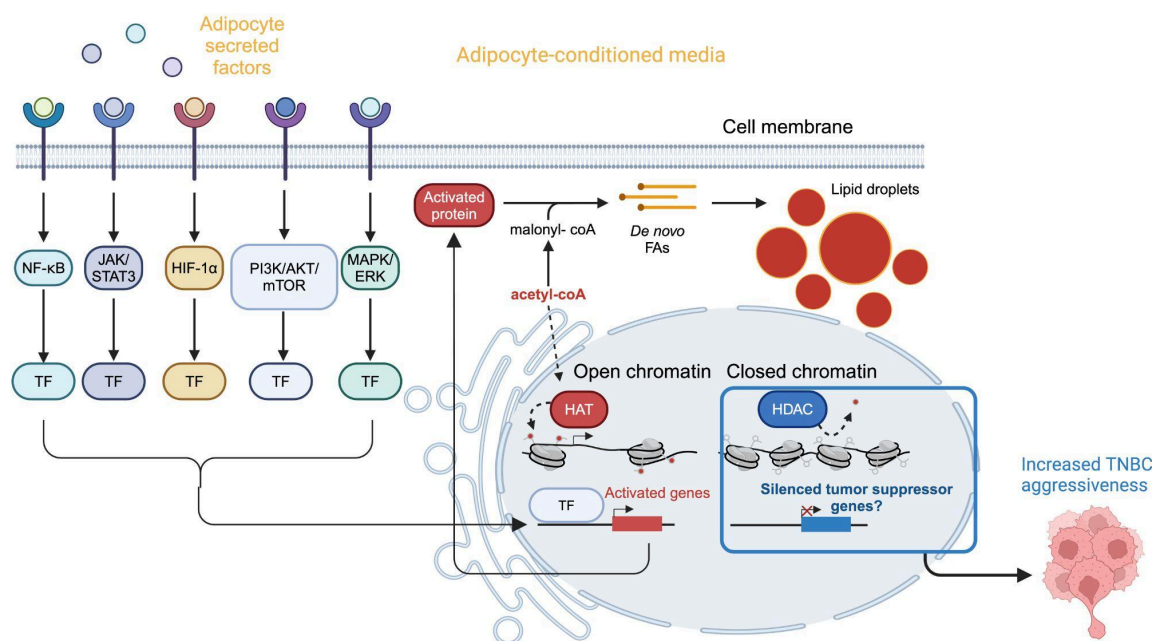


**Figure 3. Hypothesis model showing the association between lipogenesis through adipocyte secreted factor signaling and histone acetylation.**

Typically, antibodies are used to stain regions in fixed cells that have high levels of specific histone posttranslational modifications (histone PTMs) and other features such as DNA methylation and nonhistone chromatin proteins. Cells naturally express proteins called chromatin readers or reader-effectors that contain chromatin-binding domains (CBDs). Scientists have isolated the minimal CBD sequences needed to selectively bind specific histone PTMs, fused these with fluorescent proteins, and expressed these in living cells to “paint” chromatin regions in the nucleus<sup>21</sup>. This methodology has been used to detect histone acetylation (H3K14ac) in HEK293 cells<sup>22</sup>, but to our knowledge not in lipogenic breast cancer cells. Within the human BRD4 protein, a domain of 119 amino acids known as

BRD (bromodomain) specifically binds acetylated lysines within histones H3 and H4 (H3K14ac, H4K5ac, H4K8ac, H4K12ac, H4K16ac, H4K20ac)<sup>23,24</sup>. Constructs containing dimeric repeats of BRD have been shown to best colocalize with H3K14ac antibody in transfected kidney cells and provide information on the nuclear distribution of histone acetylation<sup>22</sup>. Therefore, we used a one-step DNA assembly method called Golden Gate to build a fluorescent fusion protein that contains a dimeric repeat of BRD fused to fluorescent protein with nuclear localization sequence (NLS) to visualize histone acetylation and its nuclear distribution within the nucleus of lipogenic TNBC cells.

## **Hypothesis**

Lipogenesis in triple negative breast cancer (TNBC) cells drives global loss or redistribution of histone acetylation that results in condensed (closed) chromatin that reduces the expression of tumor suppressor genes (TSGs).

## **Research Aims**

**Aim 1** - Use RNA-seq to determine the transcriptional profile of lipogenic TNBC cells and identify downregulated tumor suppressor genes (TSGs).

**Aim 2** - Use ATAC-seq to determine if chromatin takes on a condensed (closed) state at TSGs and/or other downregulated genes.

**Aim 3** - Use fusion protein technology to engineer histone acetylation reader probe to determine changes in global histone acetylation levels and nuclear distribution.

## **Methodology**

### **Cell Culture**

The BT549 cell line was grown in RPMI1640 media supplemented with 1% L-glutamine, 10% fetal bovine serum (FBS), and 0.0008 mg/mL human recombinant insulin. The BT549 cell media was used as UCM in TNBC experiments.

### **Obesity Model**

Confluent murine OP-9 bone marrow stromal cells were trypsinized and plated at  $10^5$  cells/well in 10-cm plates. Cells were cultured in DMEM media supplemented with 10% FBS. On the following day, media was changed with either fresh DMEM media supplemented with 10% FBS for stromal cell culture or insulin-oleate media (IOM, 1.8mM Oleate bound to BSA with the molar ratio of 5.5:1) for adipocyte differentiation. Supernatants from adipocytes were harvested on day 3 of culture for use as adipocyte-conditioned media (ACM) in TNBC experiments.

### **RNA-Seq**

BT-549 TNBC cells were seeded in unconditioned media (UCM) or 50% ACM, with 3 replicates per condition. We performed RNA extraction and purification for RNA-seq library preparation and deep sequencing at Novogene. RNA-seq was performed with the following parameters: paired-end, 150 bp, Q30  $\geq$  85%. We trimmed raw reads with Trim Galore and performed alignment using STAR<sup>25</sup> with the most recent human genome (GRCh38/hg38). We calculated mRNA levels and generated count matrices with RSEM<sup>26</sup>. Differential gene expression was performed with DESeq2<sup>27</sup>, using a negative binomial

distribution algorithm to recognize genes with a p-value  $\leq 0.05$  and fold change  $\geq 1.5$ . We generated a volcano plot in RStudio to show a transcriptional profile.

### **ATAC-Seq**

We prepared cell samples as in RNA-seq, and sent frozen samples to Novogene for ATAC-seq library preps and deep sequencing. We trimmed raw reads with Trim Galore and performed alignment using BWA-MEM<sup>28</sup> with the most recent human genome (GRCh38/hg38). We removed PCR duplicates using Picard. To adjust read start positions to account for Tn5 chemistry, we aligned all reads as plus (+) strands offset by +4 bp and minus (-) strands offset by -5 bp. We performed peak calling using MACS3<sup>29</sup>. We visually explored our ATAC-seq data on Integrated Genomics Viewer (IGV) to investigate chromosome accessibility near genes of interest.

### **Synthetic Reader Probe Construction**

We built a probe containing dimeric BRD repeats fused by a linker, and a fluorescent protein (FP) attached to the nuclear localization sequence (NLS). To determine which fluorescent protein allows for best quantification of histone acetylation, we built four plasmids, each containing a different fluorescent protein: yellow fluorescent protein (YFP), cyan fluorescent protein (CFP), red fluorescent protein (RFP), or green fluorescent protein (GFP). The coding sequence was inserted into an engineered mammalian vector GGDestX4. Under UCM conditions, BT-549 TNBC cells were transfected and selected under G418 to generate a stable clonal cell line. Fluorescence imaging was performed on both the

transiently transfected and stably transfected cells to determine the brightness and nuclear distribution of the fluorescence signals.

## Results

### Downregulation of tumor suppressor genes in lipogenic TNBC cells

13,724 differentially expressed transcripts of BT549 cells cultured in ACM and UCM were measured using RNA-sequencing analysis. We identified 538 upregulated differentially expressed genes (UpDEGs) in ACM compared to UCM ( $p < 0.05$ ,  $p.adj < 0.05$ , and  $FC > 1.5$ ) and 235 down regulated differentially expressed genes (DownDEGs) ( $p < 0.05$ ,  $p.adj < 0.05$ , and  $FC < -1.5$ ) (**Figure 4A**). DownDEGs are found across all chromosomes, suggesting global repression (**Figure 4B**). We then matched the downDEGs with the breast cancer TSG list BRCA from the Tumor Suppressor Gene Database (TSGene)<sup>3031</sup>. We identified 9 TSGs that were downregulated in cells treated with ACM compared to UCM: AGTR1, CDKN2C, EPHB6, IDH1, LRRC4, NFATC2, NRF1, PCDH10, and SIK1 (**Figure 4C**).

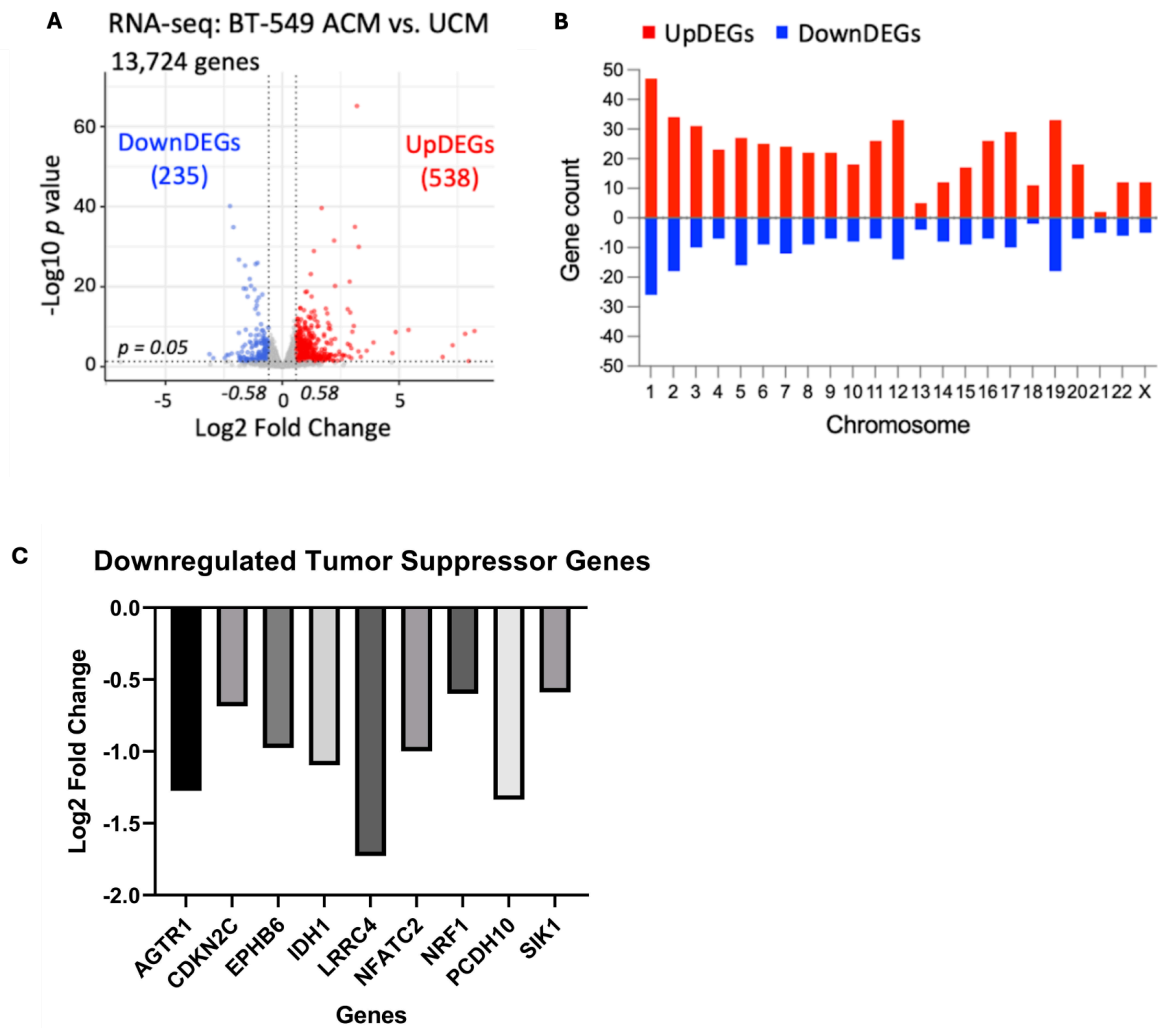


**Figure 4. Adipocyte secretome impacts the transcriptional profile of BT549 cells. (A)** Volcano plot showing upregulated and downregulated differentially expressed genes. **(B)** Differentially expressed gene distribution across all chromosomes. **(C)** Downregulated TSGs identified from RNA-seq.

**Downregulation of TSGs due to dysregulation of TFs instead of chromatin structure change**

To determine the chromosomal accessibility around the promoter site of downregulated TSGs, we loaded the six narrowPeak files and the six pileup bigWig files from ATAC-seq analysis as tracks in Integrated Genomics Viewer (IGV)<sup>31,32</sup> and selected Human (GRCh38/hg38) as genome. We navigated the window to promoter sites of all downregulated TSGs. For example, the promoter of AGTR1 is located at chr3:148697903. We looked for consistent peaks near promoter sites across all 6 narrowPeak files and 6 bigWig files (**Figure 5**), and then averaged the peak signal value of 3 ACM replicates and 3 UCM replicates respectively. Two-way ANOVA was performed on the ATAC-seq peak signal values (**Figure 6A**) and the RNA-seq TPM values (**Figure 6B**). Statistical significant difference was determined by p-value < 0.05. The peak signal value significantly increased at the promoter site of PDK4 (one of the upDEGs) for cells treated with ACM, suggesting more chromosomal accessibility for gene activation. This also tracks with RNA-seq transcript expression, as TPM of PDK4 increased in cells treated with ACM. The peak signal values of downregulated TSGs in ACM group are not significantly different from those in UCM group, suggesting no significant change in chromatin structure induced by ASFs at the promoter site of downregulated TSGs.

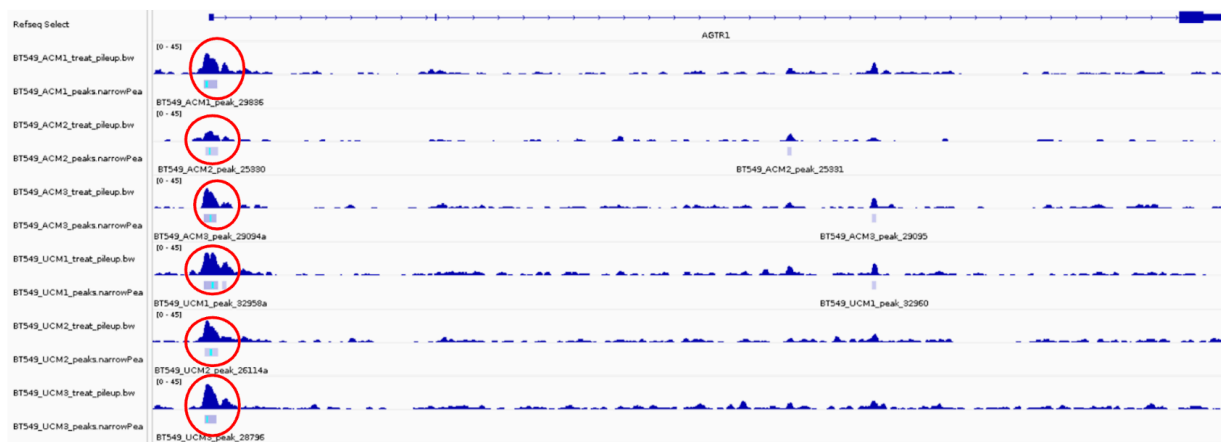


**Figure 5. Visualization of narrowPeak and bigWig files from ATAC-seq for AGTR1.**

NarrowPeak files provide called peaks of signal enrichment. BigWig files provide dense, continuous data that can be displayed on IGV as graphs. Consistency in peaks is found in all narrowPeak and bigWig files at the promoter site of AGTR1.

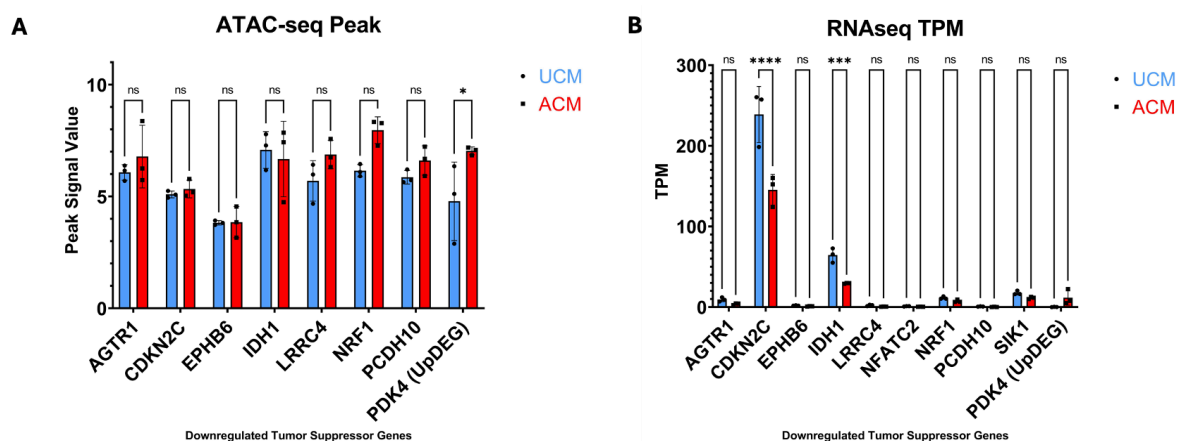


**Figure 6. Peak signal values from ATAC-seq and TPM values from RNA-seq for**

**downregulated TSGs.** (A) Peak signal values of ACM replicates are not significantly different from that of UCM replicates for downregulated TSGs. The peak signal value for PDK4 is significantly higher for cells treated with ACM. (B) RNA-seq TPM values showing transcript expression levels for downregulated TSGs and PDK4.

Our ATAC-seq analysis further suggests that the downregulation of TSGs is determined by gene regulation. Therefore, these TSGs could be regulated by a unique set of transcription factors (TFs) that are distinct from TFs that regulate the upDEGs. To test this alternative hypothesis, we performed TF binding sites enrichment analysis on upDEGs and downDEGs using TF\_targets ([https://github.com/cplaisier/TF\\_targets](https://github.com/cplaisier/TF_targets)) and the Transcription Factor Target Gene Database<sup>33</sup>. TFs were ranked based on p-value, which represents the enrichment of input genes (upDEGs or downDEGs) with TF target genes. We selected 22 TFs with most significant p-values and eliminated two TFs (SP1 and ZEB1) that target both upDEGs and downDEGs (**Figure 7A**). We then derived the top 20 most enriched unique TFs for either upDEGs or downDEGs, and determined whether the downregulated TSGs, the top 5 downDEGs and upDEGs are target genes of these TFs. As a result, downregulated TSGs and top 5 downDEGs are only targeted by most enriched TFs for downDEGs, whereas top 5 upDEGs are only targeted by most enriched TFs for upDEGs (**Figure 7B**). This suggests that the downregulation of TSGs is regulated by a specific group of TFs that exclusively regulate downDEGs.

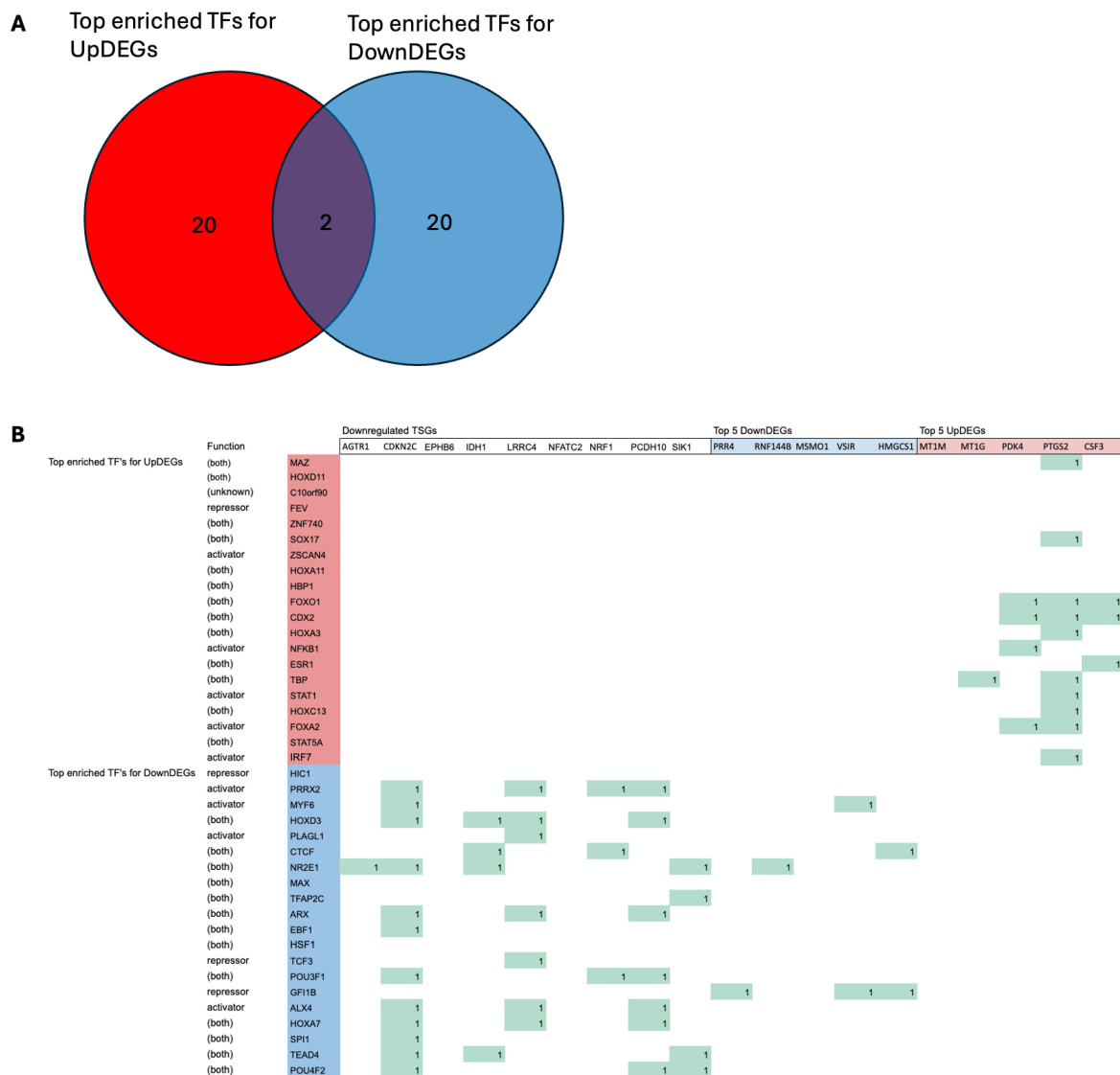


**Figure 7. Downregulated TSGs are targeted by TFs that exclusively regulate downDEGs.** (A) Venn diagram showing top 20 enriched TFs that exclusively regulate upDEGs or downDEGs. (B) DownDEGs and upDEGs are targeted by two distinct groups of TFs. Green box with “1” shows that the specific gene is targeted by that specific TF.

## Engineering Histone Acetylation Reader Probe

To prepare linear DNA donors, we performed Q5 PCR on commercial plasmids (Twist Bioscience) to add recognition sites for the Type IIS restriction enzyme BbsI and 4 bp 5' overhangs to each end of each module's open reading frame (ORF). Using the PCR products, we generated donor plasmids through Zero Blunt™ TOPO™ PCR cloning, which is a system for cloning blunt-end DNA (**Figure 8A**). Such a cloning system has several key advantages. The vector contains a kanamycin resistance gene, which is different from the ampicillin resistance gene in the GGDestX4 expression vector. This allows for the selection of cells transformed with the fully assembled Golden Gate plasmid and kills cells transformed with the donor plasmids. The PCR-Blunt II-TOPO vector also has convenient designs for plasmid donor construction validation, including recognition sites for EcoRI restriction enzyme outside donor ORF, and M13 forward and reverse primer sites for Sanger sequencing or colony PCR screening. In addition, although plasmid donors are not always necessary for Golden Gate assembly<sup>34</sup>, it allows for long-term storage and accurate regeneration of donor parts through bacterial transformation. Successful construction of plasmid donor DNA was verified by restriction digestion and Sanger sequencing.

GGDestX4 is an engineered plasmid built from pcDNA™3.1<sup>(+)</sup> neo mammalian expression vector (Thermo Fisher Scientific) that contains two modifications to make it compatible for the Golden Gate assembly (**Figure 8B**). As the expression vector must not contain any BbsI sites, Dr. Karmella Haynes performed site-directed mutagenesis to remove the BbsI site in the bovine growth hormone polyadenylation (BGH polyA) sequence of pcDNA™3.1<sup>(+)</sup> neo. Another key modification that I assisted with was linearizing the pcDNA™3.1<sup>(+)</sup> neo using restriction enzyme, and ligated with an annealed double-stranded oligo (dsOligo) containing a pair of BbsI sites for Golden Gate cloning. The dsOligo also

includes a Kozak sequence that functions as the initiation site for reader probe protein translation in eukaryotic cells<sup>35</sup>. GGDestX4 expression vector has several features that are designed for mammalian cell transfection. The CMV promoter is a strong promoter commonly used to drive transgene expression in mammalian cells<sup>36</sup>. A BGH polyA sequence allows polyA tails to be added to the mRNA transcript to terminate transcription of the reader probe<sup>37</sup>. To select for stable transfection, the GGDestX4 plasmid contains a neomycin resistance marker, which protects stable cells from the toxicity of G418. Traditionally, Golden Gate assembly requires an intermediate shuttle destination vector for the donor fragments to be assembled<sup>34</sup>. Using GGDestX4 bypasses the shuttle vector step and provides a convenient method of assembling donors directly into expression vectors.

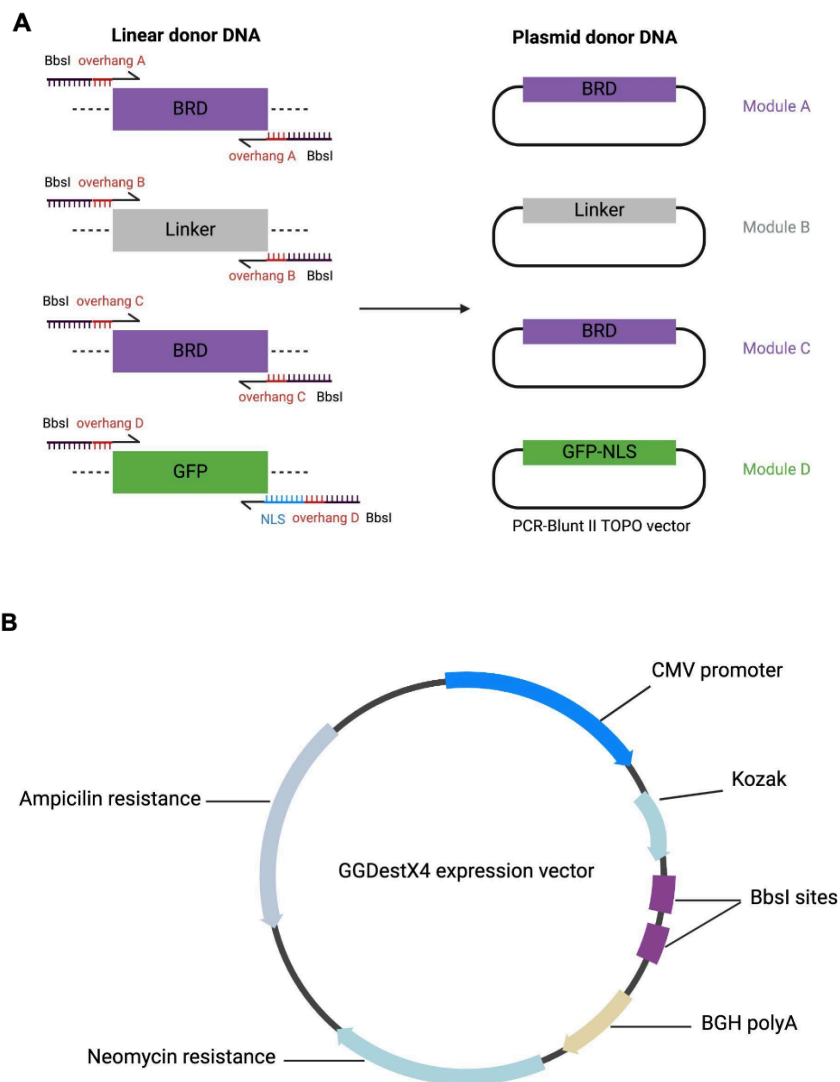


**Figure 8. Construction of Golden Gate plasmid donors and expression destination vector for histone acetylation reader probe. (A) Preparation for linear donors using PCR amplification, and plasmid donors by cloning donor DNA into PCR-Blunt II TOPO vector. GFP is used as an example for the D-part fluorescent protein. (B) Plasmid map of GGDestX4 expression vector.**

We performed Golden Gate single-pot assembly to assemble donor DNA directly into GGDestX4 expression vector. The 4 bp overhang at each end of each module's ORF guides the assembly of the four modules in order. Single-pot digestion using BbsI restriction enzyme allows the donor fragments to be cut out from PCR-Blunt II TOPO vectors, and ligated into the GGDestX4 expression vector in directed assembly (**Figure 9A**). For plasmid verification, colony PCR with MV1 primers and Sanger sequencing were performed (**Figure 9B**). For example, the expected band for plasmid 2xBRD-GFP\_GGDGX4 with complete Golden Gate assembly insert is 2625 bp.

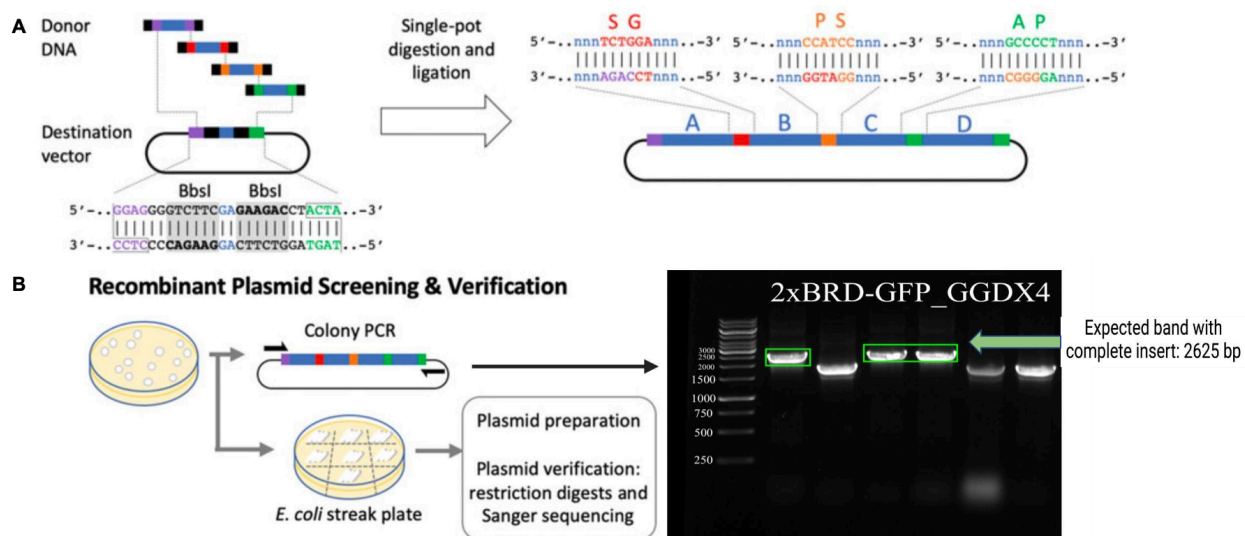


**Figure 9. Single-pot Golden Gate assembly of histone acetylation reader probe and plasmid verification.** (A) Single-pot digestion and ligation allows for directed assembly of donor modules into expression destination vector. Figure adapted from Haynes et al<sup>34</sup>. (B) Plasmid verification for Golden Gate products. The bands showing plasmids with complete Golden Gate insert for 2xBRD-GFP\_GGDGX4 are shown in green box.

The four plasmids expressing histone acetylation probes were then transfected into BT549 cells. Three days after transfection, fluorescence imaging was performed on transiently transfected cells (**Figure 10**). The overall fluorescence expression and transfected cell viability were low. To select for stable transfected cells, we added 250 ug/mL G418 to the cells. We then saw that there was an increase in cell death and the few cells expressing fluorescence did not proliferate.

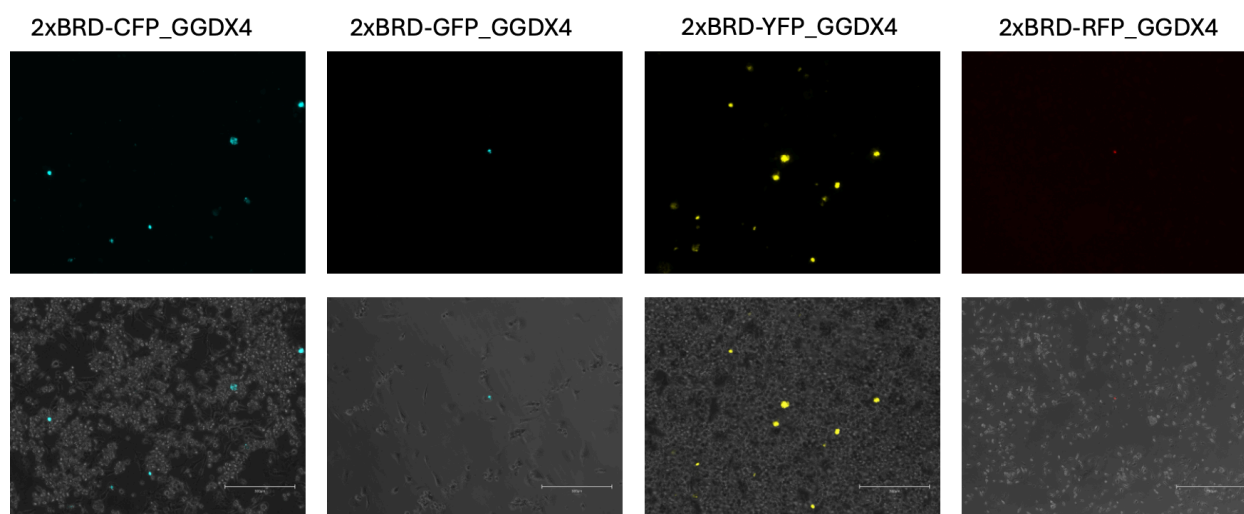


**Figure 10. Low transient transfection rate across all four histone acetylation probes.**

The first row shows imaging under CFP, GFP, YFP, and RFP channels (from left to right).

The second row shows imaging when the fluorescence channel and trans channel are merged.

## Conclusion and Future Directions

### Downregulation of TSGs induced by adipocyte secretome

In conclusion, our RNA-seq and ATAC-seq results suggest that downregulation of TSGs is not induced by change in chromosomal accessibility at the promoter site, but rather

regulated by TFs that exclusively target downDEGs. To investigate further regarding the role of TFs in TSG repression, we will treat the cells with inhibitors for specific TF that targets downregulated TSG, and measure changes in terms of cancer proliferation, metastasis, and aggressiveness. In addition, we will work with Dr. David Gorkin to normalize the ATAC-seq results in order to perform differential expression analysis, since current results are only based on signal values after peak calling.

### **Histone acetylation reader probe**

Both of the transiently transfected and stably transfected BT549 cells showed low viability of fluorescence-expressing cells. One possible explanation is that CMV, as a strong viral promoter, induces transgene silencing through CpG methylation<sup>38</sup>. The transgene expression could also be specific to cell type. Our preliminary studies have shown that HEK cells had high transfection rate with GGDestX4, but the histone acetylation probes is our first experiment transfecting GGDestX4 into TNBC cells. Instead of continuing with GGDestX4 expression vector, we will transition to the pSBtetTA-YP\_CFP vector, which is a plasmid engineered by Dr. Karmella Haynes. The pSBtetTA-YP\_CFP vector constitutively expresses YFP signals and expresses CFP when induced by doxycycline (dox) (**Figure 11**). Studies performed by graduate student Ashley Townsel have shown high transfection rates of pSBtetTA-YP\_CFP into BT549 cells under UCM conditions<sup>39</sup>. Therefore, we will make modifications to the pSBtetTA-YP\_CFP to make it compatible for Golden Gate assembly. The Golden-Gate compatible plasmid pSBtetTA-luc2GG will have CFP replaced with a Golden Gate drop-in site by ligating with annealed dsOligo to add a pair of BbsI sites for Golden Gate cloning. The constitutively expressed YFP gene will be replaced by the

colorless luciferase, as YFP's spectrum overlaps with the spectrum of GFP. We will perform site-directed mutagenesis to eliminate the BbsI site in BGH polyA and in luciferase gene.

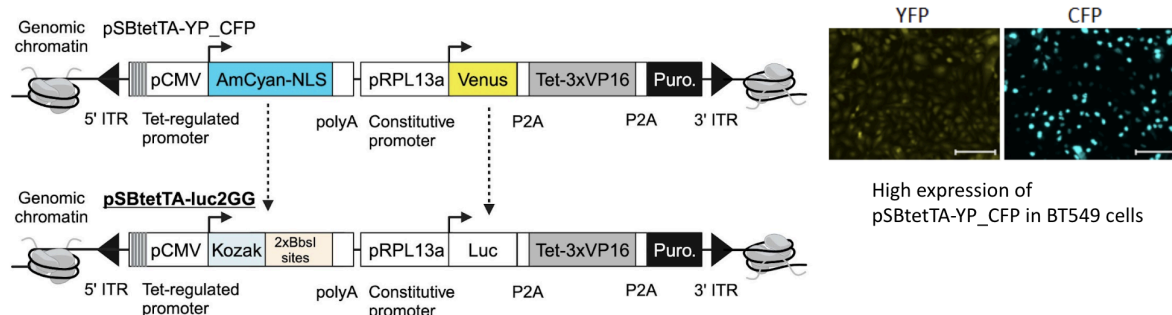


**Figure 11. Engineering design for pSBtetTA-luc2GG based on pSBtetTA-YP\_CFP.**

pSBtetTA-YP\_CFP vector constitutively expresses YFP and contains dox-inducible CFP gene. At the presence of doxycycline, Tet-TA binds to dox and undergoes a conformational change. The complex binds to the pCMV promoter, allowing CFP gene to be expressed.

After assembling the donor modules into pSBtetTA-luc2GG using Golden Gate, we will transfect the plasmids into BT549 cells and treat with dox to induce expression of the histone acetylation probe. We will then select for stable cells by adding puromycin. After generating the stably transfected cells, we will treat them with either ACM or UCM to determine how ASFs impact the fluorescence brightness and nuclear distribution of histone acetylation. We will also have a positive control where cells are treated with histone deacetyltransferase (HDAC) inhibitor, and a negative control where cells are treated with histone acetyltransferase (HAT) inhibitor. We expect to see diffuse fluorescence expression in cells treated with ACM or HAT inhibitor (HATi), as the synthetic reader probes are expressed but do not bind to acetylated histone lysine tails. In cells treated with UCM or HDAC inhibitor (HDACi), we expect to see concentrated fluorescence expression, due to

higher concentration in histone acetylation in some regions of the nucleus than the others (Figure 12).

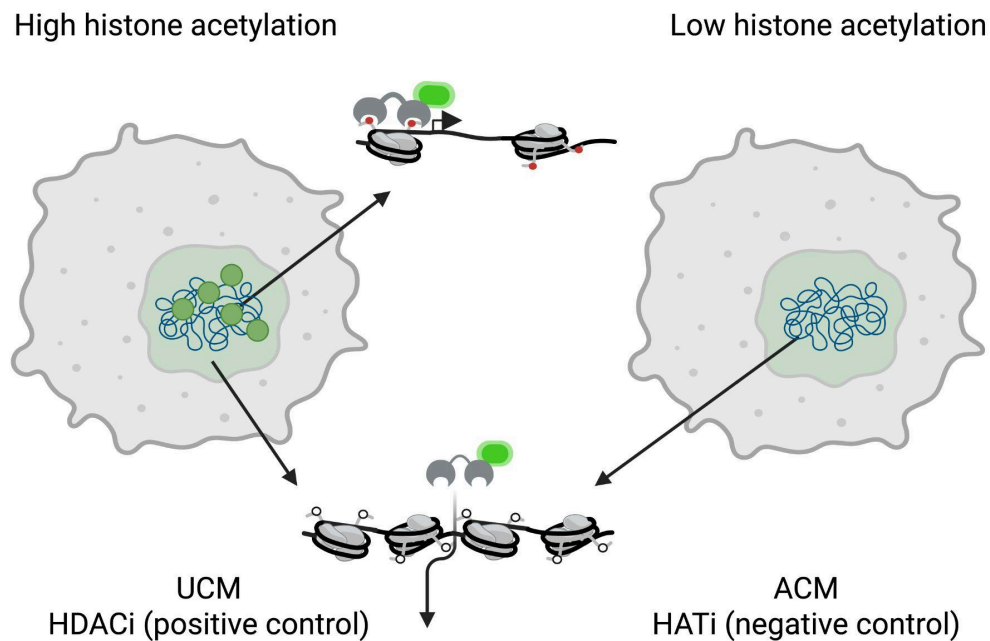


**Figure 12. Expected results of fluorescence expression in stably transfected BT549 cells treated with different conditions.** Using 2xBRD-GFP\_GGDX4 as an example, we expect to see diffuse GFP expression in cells treated with ACM or HATi, while concentrated GFP expression is expected in cells treated with UCM or HDACi.

## References

1. Hales CM, Carroll MD, Fryar CD, Ogden CL. Prevalence of Obesity and Severe Obesity Among Adults: United States, 2017-2018. NCHS Data Brief. 2020 Feb;(360):1–8. PMID: 32487284
2. Hurt RT, Kulisek C, Buchanan LA, McClave SA. The obesity epidemic: challenges, health initiatives, and implications for gastroenterologists. Gastroenterol Hepatol (N

- Y). 2010 Dec;6(12):780–792. PMID: PMC3033553
3. Avgerinos KI, Spyrou N, Mantzoros CS, Dalamaga M. Obesity and cancer risk: Emerging biological mechanisms and perspectives. *Metabolism*. 2019 Mar;92:121–135. PMID: 30445141
  4. Bray F, Ferlay J, Soerjomataram I, Siegel RL, Torre LA, Jemal A. Global cancer statistics 2018: GLOBOCAN estimates of incidence and mortality worldwide for 36 cancers in 185 countries. *CA Cancer J Clin*. 2018 Nov;68(6):394–424. PMID: 30207593
  5. Rakha EA, El-Sayed ME, Green AR, Lee AHS, Robertson JF, Ellis IO. Prognostic markers in triple-negative breast cancer. *Cancer*. 2007 Jan 1;109(1):25–32. PMID: 17146782
  6. Sun H, Zou J, Chen L, Zu X, Wen G, Zhong J. Triple-negative breast cancer and its association with obesity. *Mol Clin Oncol*. 2017 Dec;7(6):935–942. PMID: PMC5740844
  7. Widschwendter P, Friedl TW, Schwentner L, DeGregorio N, Jaeger B, Schramm A, Bekes I, Deniz M, Lato K, Weissenbacher T, Kost B, Andergassen U, Jueckstock J, Neugebauer J, Trapp E, Fasching PA, Beckmann MW, Schneeweiss A, Schrader I, Rack B, Janni W, Scholz C. The influence of obesity on survival in early, high-risk breast cancer: results from the randomized SUCCESS A trial. *Breast Cancer Res*. 2015 Sep 18;17(1):129. PMID: PMC4575482
  8. Lennon H, Sperrin M, Badrick E, Renehan AG. The Obesity Paradox in Cancer: a

- Review. *Curr Oncol Rep*. 2016 Sep;18(9):56. PMID: PMC4967417
9. Simeone P, Tacconi S, Longo S, Lanuti P, Bravaccini S, Pirini F, Ravaioli S, Dini L, Giudetti AM. Expanding Roles of De Novo Lipogenesis in Breast Cancer. *Int J Environ Res Public Health* [Internet]. 2021 Mar 30;18(7). Available from: <http://dx.doi.org/10.3390/ijerph18073575> PMID: PMC8036647
  10. Gourgue F, Mignon L, Van Hul M, Dehaen N, Bastien E, Payen V, Leroy B, Joudiou N, Vertommen D, Bouzin C, Delzenne N, Gallez B, Feron O, Jordan BF, Cani PD. Obesity and triple-negative-breast-cancer: Is apelin a new key target? *J Cell Mol Med*. 2020 Sep;24(17):10233–10244. PMID: PMC7520321
  11. Suleiman JB, Mohamed M, Bakar ABA. A systematic review on different models of inducing obesity in animals: Advantages and limitations. *J Adv Vet Anim Res*. 2020 Mar;7(1):103–114. PMID: PMC7096124
  12. Takahashi H, McCaffery JM, Irizarry RA, Boeke JD. Nucleocytosolic acetyl-coenzyme a synthetase is required for histone acetylation and global transcription. *Mol Cell*. 2006 Jul 21;23(2):207–217. PMID: 16857587
  13. Cruz ALS, Barreto E de A, Fazolini NPB, Viola JPB, Bozza PT. Lipid droplets: platforms with multiple functions in cancer hallmarks. *Cell Death Dis*. 2020 Feb 6;11(2):105. PMID: PMC7005265
  14. Nickel A, Blücher C, Kadri OA, Schwagarus N, Müller S, Schaab M, Thiery J, Burkhardt R, Stadler SC. Adipocytes induce distinct gene expression profiles in mammary tumor cells and enhance inflammatory signaling in invasive breast cancer

- cells. *Sci Rep.* 2018 Jun 21;8(1):9482. PMID: PMC6013441
15. Gyamfi J, Lee YH, Eom M, Choi J. Interleukin-6/STAT3 signalling regulates adipocyte induced epithelial-mesenchymal transition in breast cancer cells. *Sci Rep.* 2018 Jun 11;8(1):8859. PMID: PMC5995871
  16. Shah T, Krishnamachary B, Wildes F, Mironchik Y, Kakkad SM, Jacob D, Artemov D, Bhujwala ZM. HIF isoforms have divergent effects on invasion, metastasis, metabolism and formation of lipid droplets. *Oncotarget.* 2015 Sep 29;6(29):28104–28119. PMID: PMC4695047
  17. Yadav S, Virk R, Chung CH, Eduardo MB, VanDerway D, Chen D, Burdett K, Gao H, Zeng Z, Ranjan M, Cottone G, Xuei X, Chandrasekaran S, Backman V, Chatterton R, Khan SA, Clare SE. Lipid exposure activates gene expression changes associated with estrogen receptor negative breast cancer. *NPJ Breast Cancer.* 2022 May 4;8(1):59. PMID: PMC9068822
  18. Rios Garcia M, Steinbauer B, Srivastava K, Singhal M, Mattijssen F, Maida A, Christian S, Hess-Stumpp H, Augustin HG, Müller-Decker K, Nawroth PP, Herzig S, Berriel Diaz M. Acetyl-CoA Carboxylase 1-Dependent Protein Acetylation Controls Breast Cancer Metastasis and Recurrence. *Cell Metab.* 2017 Dec 5;26(6):842–855.e5. PMID: 29056512
  19. Cai L, Sutter BM, Li B, Tu BP. Acetyl-CoA induces cell growth and proliferation by promoting the acetylation of histones at growth genes. *Mol Cell.* 2011 May 20;42(4):426–437. PMID: PMC3109073

20. Zhuang J, Huo Q, Yang F, Xie N. Perspectives on the Role of Histone Modification in Breast Cancer Progression and the Advanced Technological Tools to Study Epigenetic Determinants of Metastasis. *Front Genet.* 2020 Oct 29;11:603552. PMID: PMC7658393
21. Gray S. *Epigenetic Cancer Therapy.* Elsevier; 2023.
22. Sanchez OF, Mendonca A, Carneiro AD, Yuan C. Engineering Recombinant Protein Sensors for Quantifying Histone Acetylation. *ACS Sens.* 2017 Mar 24;2(3):426–435. PMID: 28723212
23. Filippakopoulos P, Picaud S, Mangos M, Keates T, Lambert JP, Barsyte-Lovejoy D, Felletar I, Volkmer R, Müller S, Pawson T, Gingras AC, Arrowsmith CH, Knapp S. Histone recognition and large-scale structural analysis of the human bromodomain family. *Cell.* 2012 Mar 30;149(1):214–231. PMID: PMC3326523
24. Wang R, You J. Mechanistic analysis of the role of bromodomain-containing protein 4 (BRD4) in BRD4-NUT oncoprotein-induced transcriptional activation. *J Biol Chem.* 2015 Jan 30;290(5):2744–2758. PMID: PMC4317035
25. Dobin A, Davis CA, Schlesinger F, Drenkow J, Zaleski C, Jha S, Batut P, Chaisson M, Gingeras TR. STAR: ultrafast universal RNA-seq aligner. *Bioinformatics.* 2013 Jan 1;29(1):15–21. PMID: PMC3530905
26. Li B, Dewey CN. RSEM: accurate transcript quantification from RNA-Seq data with or without a reference genome. *BMC Bioinformatics.* 2011 Aug 4;12:323. PMID: PMC3163565

27. Love MI, Huber W, Anders S. Moderated estimation of fold change and dispersion for RNA-seq data with DESeq2. *Genome Biol.* 2014;15(12):550. PMID: PMC4302049
28. Li H, Durbin R. Fast and accurate short read alignment with Burrows-Wheeler transform. *Bioinformatics.* 2009 Jul 15;25(14):1754–1760. PMID: PMC2705234
29. Zhang Y, Liu T, Meyer CA, Eeckhoute J, Johnson DS, Bernstein BE, Nusbaum C, Myers RM, Brown M, Li W, Liu XS. Model-based analysis of ChIP-Seq (MACS). *Genome Biol.* 2008 Sep 17;9(9):R137. PMID: PMC2592715
30. Zhao M, Sun J, Zhao Z. TSGene: a web resource for tumor suppressor genes. *Nucleic Acids Res.* 2013 Jan;41(Database issue):D970–6. PMID: PMC3531050
31. Zhao M, Kim P, Mitra R, Zhao J, Zhao Z. TSGene 2.0: an updated literature-based knowledgebase for tumor suppressor genes. *Nucleic Acids Res.* 2016 Jan 4;44(D1):D1023–31. PMID: PMC4702895
32. Robinson JT, Thorvaldsdóttir H, Winckler W, Guttman M, Lander ES, Getz G, Mesirov JP. Integrative genomics viewer. *Nat Biotechnol.* 2011 Jan;29(1):24–26. PMID: PMC3346182
33. Plaisier CL, O'Brien S, Bernard B, Reynolds S, Simon Z, Toledo CM, Ding Y, Reiss DJ, Paddison PJ, Baliga NS. Causal Mechanistic Regulatory Network for Glioblastoma Deciphered Using Systems Genetics Network Analysis. *Cell Syst.* 2016 Aug;3(2):172–186. PMID: PMC5001912
34. Haynes KA, Priode JH. Rapid Single-Pot Assembly of Modular Chromatin Proteins for

- Epigenetic Engineering. *Methods Mol Biol.* 2023;2599:191–214. PMID: 36427151
35. Khalid K, Poh CL. The development of DNA vaccines against SARS-CoV-2. *Adv Med Sci.* 2023 Sep;68(2):213–226. PMID: PMC10290423
36. Radhakrishnan P, Basma H, Klinkebiel D, Christman J, Cheng PW. Cell type-specific activation of the cytomegalovirus promoter by dimethylsulfoxide and 5-aza-2'-deoxycytidine. *Int J Biochem Cell Biol.* 2008 Mar 7;40(9):1944–1955. PMID: PMC4011493
37. Wang XY, Du QJ, Zhang WL, Xu DH, Zhang X, Jia YL, Wang TY. Enhanced Transgene Expression by Optimization of Poly A in Transfected CHO Cells. *Front Bioeng Biotechnol.* 2022 Jan 24;10:722722. PMID: PMC8819543
38. Cabrera A, Edelstein HI, Glykofrydis F, Love KS, Palacios S, Tycko J, Zhang M, Lensch S, Shields CE, Livingston M, Weiss R, Zhao H, Haynes KA, Morsut L, Chen YY, Khalil AS, Wong WW, Collins JJ, Rosser SJ, Polizzi K, Elowitz MB, Fussenegger M, Hilton IB, Leonard JN, Bintu L, Galloway KE, Deans TL. The sound of silence: Transgene silencing in mammalian cell engineering. *Cell Syst.* 2022 Dec 21;13(12):950–973. PMID: PMC9880859
39. Townsel, A., Wu, Y., Jaffe, M., Shields, C., & Haynes, K. A. (2024). Tet Transgene Activation is Disrupted in Lipogenic Triple Negative Breast Cancer Cells. *bioRxiv*, 2024-10.